

THE WEIGHTED LEAST SQUARE SCHEME FOR MULTIDIMENSIONAL FLOWS

Jiří Fůrst*

*Czech Technical University in Prague, Faculty of Mechanical Engineering
 Karlovo nám. 13, 121 35, Praha
 Czech Republic
 e-mail: Jiri.Furst@fs.cvut.cz

Key words: Compressible flows, Finite volume method, essentially non-oscillatory schemes

Abstract. *This article describes the development of a high order finite volume method for the solution of transonic flows. The high order of accuracy is achieved by a reconstruction procedure similar to the weighted essentially non-oscillatory schemes (WENO). On the contrary to the WENO schemes, the weighted least square (WLSQR) scheme is easily extensible to the case of complex geometry.*

1 INTRODUCTION

This article deals with the numerical solution of the Euler or the Navier–Stokes equations describing the motion of compressible inviscid or viscous gas

$$\frac{\partial \rho}{\partial t} + \frac{\partial}{\partial x_j} (\rho v_j) = 0, \tag{1}$$

$$\frac{\partial}{\partial t} (\rho v_i) + \frac{\partial}{\partial x_j} (\rho v_i v_j) + \frac{\partial p}{\partial x_i} = \frac{\partial \tau_{ij}}{\partial x_j}, \tag{2}$$

$$\frac{\partial E}{\partial t} + \frac{\partial}{\partial x_j} ((E + p)v_j) = \frac{\partial}{\partial x_j} (v_i \tau_{ij}) - \frac{\partial q_j}{\partial x_j}, \tag{3}$$

where ρ is the density, v_i are the components of the velocity vector, p is the pressure, E is the total energy per volume unit, τ_{ij} is the stress tensor, and q_j are the components of heat flux¹.

The solution can be obtained with a standard finite volume method. However, the basic method of Godunov type often suffers from low accuracy. One possibility how to improve the accuracy of such method is the application of an interpolation procedure which tries to reconstruct pointwise values of the solution from their cell averages. The main problem of such interpolation procedures is their applicability for data with discontinuities and/or strong gradients. The so called ENO (i.e. *essentially non-oscillatory*) reconstruction has been developed^{2;3} and transformed to finite volumes by many researchers at the end of

last century. Nevertheless, the standard finite volume version of ENO or weighted ENO method^{4;5} is relatively complicated for general meshes. On the other hand, the proposed WLSQR interpolation is simply extendible also for 3D (see last section of this article for an example).

The reconstruction procedure based on the least square method combined with data dependent weights for avoiding interpolation across a discontinuity has been developed⁶. The article⁶ presents several applications of the original weighted least square method with piecewise linear reconstruction namely for inviscid transonic flows in 2D channels and turbine cascades. The extension to the piecewise parabolic interpolation for scalar test case has been done later⁷ and the analysis of the stability of proposed interpolation method has been studied in the articles^{8;9}.

The aim of this article is to present some numerical experiments concerning the choice of the weights in the reconstruction and to test the method in 2D and 3D both for flows with complex structure (2D Riemann problem), and for flows in complex geometries.

2 THE HIGH ORDER FINITE VOLUME SCHEME

As a base for the numerical method the standard finite volume method with data located in centers of polygonal cells has been chosen. The basic low order semi-discrete method can be written as¹

$$\frac{du_i(t)}{dt} = - \sum_{j \in \mathcal{N}_i} \mathcal{F}(u_i(t), u_j(t), \vec{S}_{ij}). \quad (4)$$

Here $u_i(t)$ is the averaged solution over a cell C_i , \mathcal{N}_i denotes the set of indices of neighborhoods of C_i (i.e. if $j \in \mathcal{N}_i$, then cells C_i and C_j share an edge in 2D or a face in 3D), \vec{S}_{ij} is the scaled normal vector to the interface between C_i and C_j (oriented to C_j) and \mathcal{F} denotes the so called numerical flux approximating physical flux through the interface between cells C_i and C_j . The Osher's¹⁰ or AUSMPW+¹¹ fluxes were chosen in this work, nevertheless the other choice of the numerical flux (e.g. Roe's flux etc) is possible.

A higher order method can be obtained by introducing a cell-wise interpolation $P(\vec{x}; u) = P_i(\vec{x}; u)$ for $x \in C_i$ into the basic formula. The higher order method is then formally

$$\frac{du_i(t)}{dt} = - \sum_{j \in \mathcal{N}_i} \mathcal{F}(P_i(\vec{x}_{ij}; u), P_j(\vec{x}_{ij}; u), \vec{S}_{ij}), \quad (5)$$

where \vec{x}_{ij} is the center of interface between C_i and C_j .

The semi-discrete is then solved either by explicit Runge-Kutta method, either by implicit backward Euler method^{12;7}.

3 THE WEIGHTED LEAST SQUARE RECONSTRUCTION

The very important part of the above mentioned method is the high order reconstruction (or interpolation). The reconstruction should satisfy following requirements:

1. **Conservativity**, i.e. the mean value of the interpolant $P(x; u)$ over any cell C_i should be equal to cell average of u , in other words

$$\int_{C_i} P(\vec{x}; u) d\vec{x} = |C_i|u_i. \quad (6)$$

2. **Accuracy**, i.e. for a given smooth function $\tilde{u}(\vec{x})$ with cell averages u_i the interpolant $P(\vec{x}; u)$ should approximate \tilde{u} :

$$P(\vec{x}; u) = \tilde{u}(\vec{x}) + \mathcal{O}(h^o), \quad (7)$$

where h is a characteristic mesh size and o is the order of accuracy. This accuracy requirement is reformulated in the following way: let \mathcal{M}_i denotes a set of indices of cells in the vicinity of C_i (the \mathcal{M}_i will be described later). Then the prolongation of $P_i(\vec{x}; u)$ over cells given by \mathcal{M}_i should satisfy

$$\int_{C_j} P_i(\vec{x}; u) d\vec{x} = |C_j|u_j, \quad \forall j \in \mathcal{M}_i. \quad (8)$$

3. **Non-oscillatory**, i.e. the total variation of the interpolant should be bounded for $h \rightarrow 0$.

As soon as the set \mathcal{M}_i contains sufficient number of cell indices, the system becomes overdetermined and it is solved by the means of least square method. The interpolant $P_i(\vec{x}; u)$ is therefore obtained by minimizing error in (7) for $j \in \mathcal{M}_i$ respect to constraint (6). In order to mimic weighted ENO method the data dependent weights are introduced:

$$P_i(\vec{x}; u) = \arg \min \sum_{j \in \mathcal{N}_i} \left[w_{ij} \left(\int_{C_j} \tilde{P}(\vec{x}; u) d\vec{x} - |C_j|u_j \right) \right]^2, \quad (9)$$

where minimum is take over all linear polynomials \tilde{P} satisfying (6), in other words, P_i is defined as a polynomial satisfying (6) and minimizing errors in (8) in L_2 norm. Weights w_{ij} should depend on u and they should be high when u is smooth and small when there is a discontinuity in u . This behavior is similar to ENO reconstruction which can be for piecewise linear polynomials in 1D written as WLSQR reconstruction with weights being either 1 or 0. In this case, the weights

$$w_{ij} = \sqrt{\frac{h^{-r}}{\left| \frac{u_i - u_j}{h} \right|^p + h^q}}, \quad (10)$$

with p , q , and r being constants (e.g. $p = 4$, $q = -2$, $r = 3$) were chosen.

Another question is the choice of fixed stencil (denoted here by \mathcal{M}_i). The two types of stencils were used in this work for piecewise linear interpolations:

the compact stencil - $\mathcal{M}_i = \mathcal{M}_i^c$ is the set of cells sharing with C_i an edge (or face in 3D), and

the wide stencil - $\mathcal{M}_i \mathcal{M}_i^w$ is the set of cells sharing at least one vertex with C_i .

For a piecewise parabolic reconstruction the stencils are

the compact stencil - $\mathcal{M}_i = \cup_{j \in \mathcal{M}_i^c} \mathcal{M}_j^c$, and

the wide stencil - $\mathcal{M}_i = \cup_{j \in \mathcal{M}_i^w} \mathcal{M}_j^w$.

Note, that for system of equation the polynomial reconstruction is made component-wise.

3.1 Analysis of weights in WLSQR interpolation

The complete analysis of this three-parametric family of weights is very difficult task, therefore we investigate here only effects of p and q . The value of r was kept constant $r = 3$ in this work.

The theoretical analysis of 1D piecewise linear reconstruction using a regular mesh has been done in⁹ following results:

Theorem 1 *Assume a sufficiently smooth function $u(x)$ having cell averages u_i and weights $w \neq 0$. Then the piecewise linear WLSQR interpolation polynomial approximates $u(x)$ with second order of accuracy, i.e.*

$$P(x; u) = u(x) + \mathcal{O}(h^2). \quad (11)$$

In the case of discontinuous data the total variation of the interpolant for $u(x)$ defined as $u(x) = 1$ for $x < x_{shock}$ and $u(x) = 0$ for $x \geq x_{shock}$ has been analyzed and the following estimate has been proven for $p + q \geq 0$ and $p > 1$:

$$TV(P(x; u)) \leq TV(u) + 6h^{1+q/p}. \quad (12)$$

This yields the following lemma:

Theorem 2 *Assume weights with*

$$p + q \geq 0, \quad (13)$$

$$p > 0. \quad (14)$$

Then the total variation of the interpolant of data given by a single shock with constant states at both sides will be bounded independently of h as $h \rightarrow 0$.

Several numerical experiments for piecewise linear WLSQR method were described in¹³ with the conclusion that the choices $p, q, r = 4, -2, 3$ or $4, -3, 3$ are appropriate at least for inviscid transonic flows in test channel.

4 THE APPLICATIONS FOR COMPRESSIBLE FLOWS

4.1 Inviscid transonic flow through 2D test channel

As a first test of high order WLSQR scheme the flows through 2D channel with circular bump with 10% height was solved. This is well known GAMM channel and it is used by many authors for validation. The flow is characterized by the ratio of outlet static pressure and inlet stagnation pressure $p_{out}/p_{0,in} = 0.737$ corresponding to the outle isentropic Mach number $M_{2i} = 0.675$. Several calculations using the same Osher’s numerical flux¹⁰ and:

- base scheme without any reconstruction,
- scheme with piecewise linear WLSQR reconstruction, and
- scheme with piecewise parabolic WLSQR reconstruction

were performed. Each calculation has been done on three different structured meshes: the coarse mesh with 75×25 cells, intermediate mesh with 150×50 cells, and fine mesh with 300×100 cells. No mesh refining has been used, so the mesh spacing Δx was constant over whole mesh and Δy was constant at each grid line. Steady state solution was reached in all cases in less than 300 iterations of backward Euler semi-implicit method (see fig. 1). Note, that the norm of residual goes down to the level of machine zero which is usually not the case of methods with limiters (e.g. the Barth’s limiter). In order to test the applicability for the case of complex geometries another calculation with unstructured mesh with 22544 triangles refined near leading and trailing edges and in the vicinity of the shock was performed.

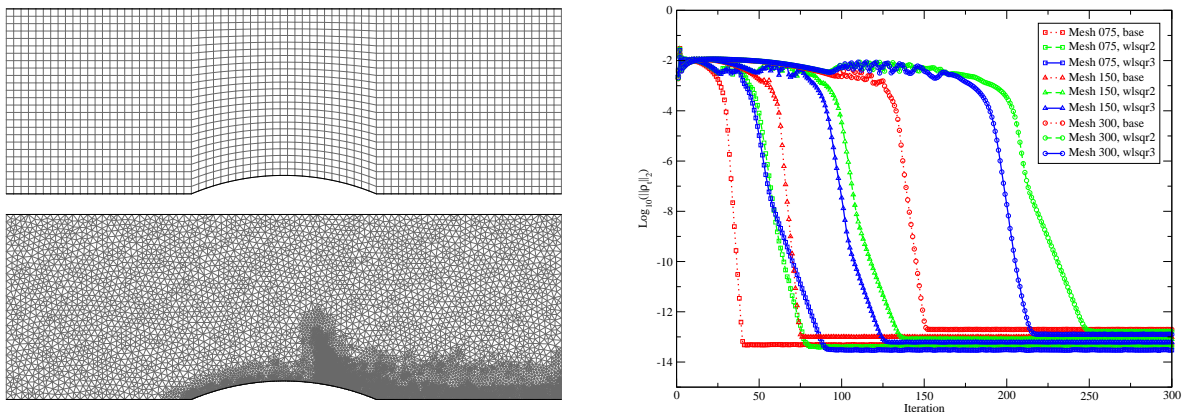


Figure 1: Coarse and unstructured meshes and convergence history for 2D test channel.

Figure 2 shows distribution of Mach number and entropy $s = \ln(p) - \gamma \ln(\rho)$ along the lower wall. One can see that the scheme without any reconstruction underestimates the maximal Mach number and moves the position of the shock little-bit upstream even in

the case of fine mesh. On the other hand, both second and third order schemes give very similar results. Very interesting comparison is the distribution of entropy along lower wall. The first order scheme shows very intensive non-physical growth of entropy at the leading and trailing edges of the bump due to strong numerical dissipation. This entropy growth is much smaller for second and third order scheme. The third order scheme with refined unstructured mesh shows almost no sources of entropy near leading and trailing edges.

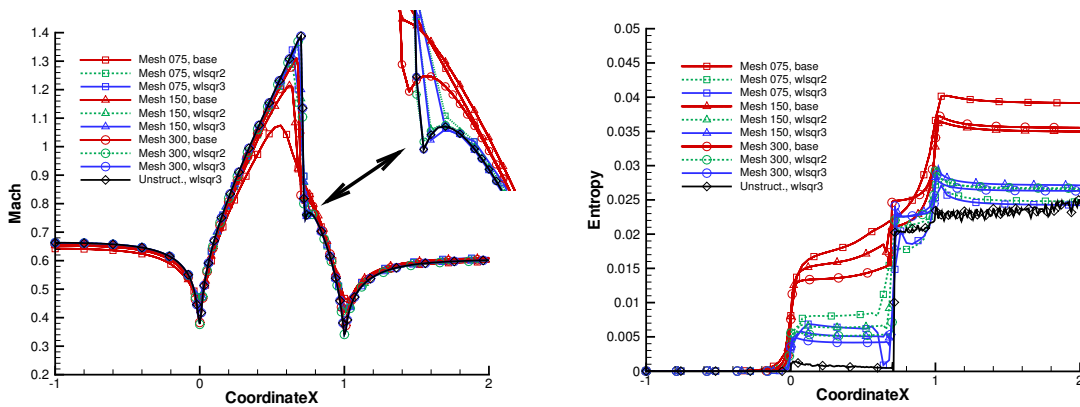


Figure 2: Distribution of Mach number and entropy along lower wall of GAMM channel; first order (dotted), second order (dashed) and third order (solid) scheme; coarse (75, rectangles), intermediate (150 × 50 triangles), fine (300 × 100, circles), and unstructured (diamonds) mesh.

In order to estimate numerically order of convergence we compute norms of $\|\rho_h - P_{h/2}^h \rho_{h/2}\|_1$ and $\|\rho_{h/2} - P_{h/4}^{h/2} \rho_{h/4}\|_1$ where ρ_h is the density obtained on coarse mesh, $\rho_{h/2}$ on the intermediate mesh, and $\rho_{h/4}$ on the fine mesh. Projection $P_{h/2}^h$ transfers solution from intermediate to coarse mesh and $P_{h/4}^{h/2}$ from fine to intermediate mesh. The order of convergence is then estimated as

$$p = \log_2(\|\rho_h - P_{h/2}^h \rho_{h/2}\|_1) - \log_2(\|\rho_{h/2} - P_{h/4}^{h/2} \rho_{h/4}\|_1). \quad (15)$$

Table 1 shows estimated orders of convergence for this case. The parabolic reconstruction (i.e. the so-called third order scheme) gives numerically only order $p = 1.3$. Nevertheless, the magnitude of the difference is still smaller than for the second order scheme. Similar deficit of order of convergence was already found in simple scalar case⁷, although here it can be caused also by the fact, that the boundary was approximated by simple straight segments. This simplification introduces error of the order h^2 into the method.

Reconstruction	$\ \rho_h - P_{h/2}^h \rho_{h/2}\ _1$	$\ \rho_{h/2} - P_{h/4}^{h/2} \rho_{h/4}\ _1$	order
None	$6.779 \cdot 10^{-3}$	$3.620 \cdot 10^{-3}$	0.90
Linear	$1.353 \cdot 10^{-3}$	$4.895 \cdot 10^{-4}$	1.46
Parabolic	$1.079 \cdot 10^{-3}$	$4.378 \cdot 10^{-4}$	1.30

Table 1: Estimated orders of convergence for GAMM channel benchmark

4.2 Two-dimensional Riemann problem

The two-dimensional Riemann problem defined by its initial state

$$\rho, u, v, p = \begin{cases} 1.5, & 0.0, & 0.0, & 1.5, & \text{for } x \geq 0.8, y \geq 0.8, \\ 0.532258, & 0.0, & 1.206045, & 0.3, & \text{for } x \geq 0.8, y < 0.8, \\ 0.532258, & 1.206045, & 0.0, & 0.3, & \text{for } x < 0.8, y \geq 0.8, \\ 0.137993, & 1.206045, & 1.206045, & 0.029032, & \text{for } x < 0.8, y < 0.8, \end{cases} \quad (16)$$

has been chosen as a very complicated test of the stability and accuracy of the WLSQR method. It is one of the two-dimensional Riemann problems studied by Kurganov and Tadmor¹⁴ Dobeš and Deconinck¹⁵ and others. The flow structure is very complex, the interaction of the shocks generates two symmetric lambda-shaped couples of shocks and a downward moving normal shock. A pair of very strong slip lines emanate from the lower triple points and interact with one of the branches of the lambda-shocks, while a jet of fluid is pushed from the right-upper corner against the normal shock (see fig. 3).

The problem is time-dependent and therefore the third order TVD Runge-Kutta has been chosen for discretization in time. The solution was computed using two unstructured meshes, coarse one with 79024 triangles and fine with 316864 triangles inside a rectangular domain $\Omega = [0, 1] \times [0, 1]$. It corresponds to the average edge lengths $h = 1/200$ and $h = 1/400$ respectively.

The “standard” choice of the weight in WLSQR scheme (i.e. weights given by (10) with $p, q, r = 4, -2, 3$) was not appropriate for this case. The solution given at the figure 3 was obtained using the weights

$$w_{ij} = \sqrt{\frac{h^{-r}}{\left|\frac{u_i - u_j}{h}\right|^p + \epsilon h^q}}, \quad (17)$$

with $p = 2, q = -1, r = 2, \epsilon = 10^{-6}$.

4.3 Turbulent flow through a 2D turbine cascade

As an example of industrial application of the WLSQR method the turbulent transonic through 2D turbine cascade has been solved. The RANS equations are equipped by the two-equation TNT $k - \omega$ model of Kok¹⁶. The values of the stagnation pressure, the stagnation temperature, the angle of attack, the turbulent intensity, and the turbulent

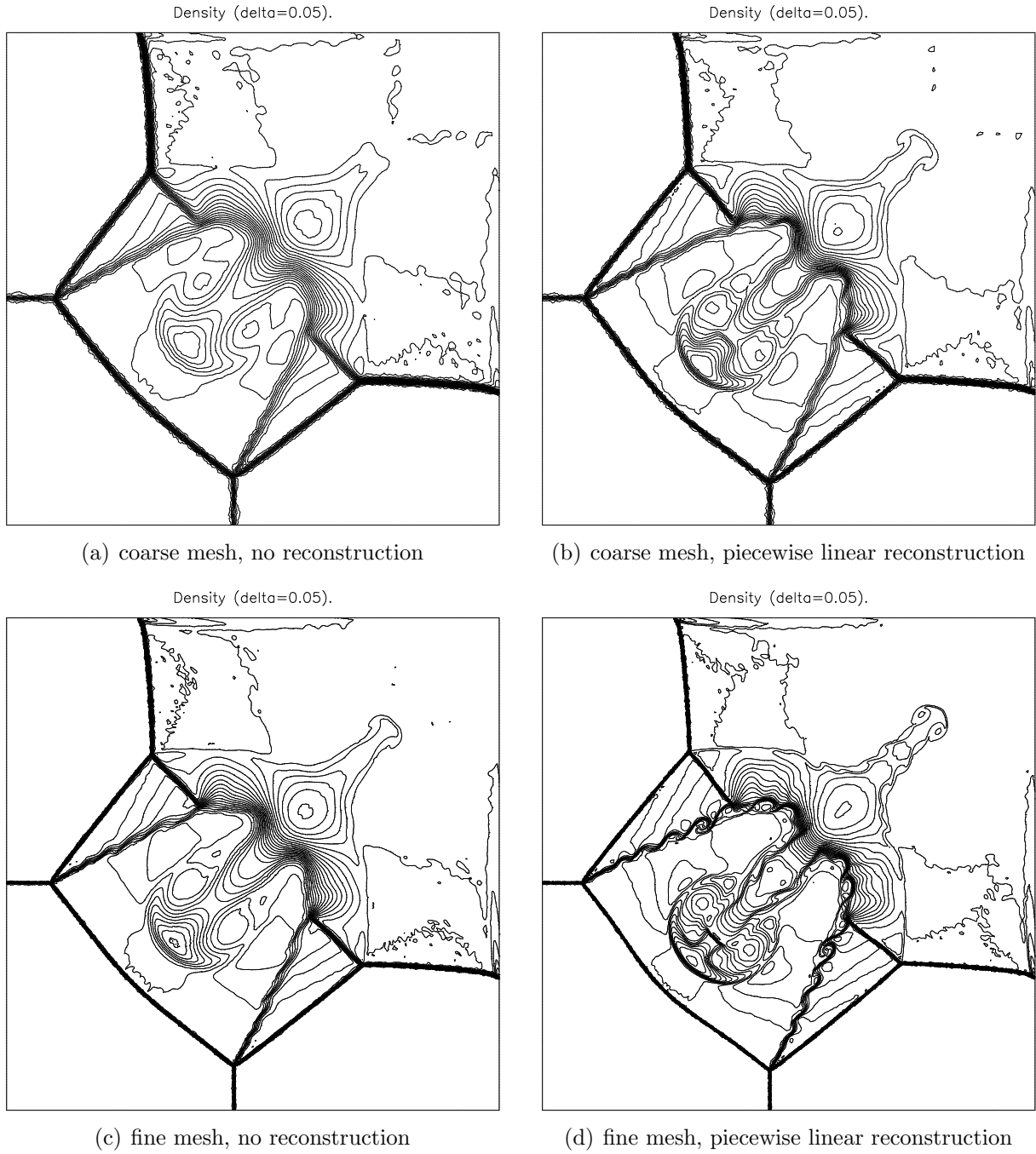


Figure 3: Isolines of density for 2D Riemann problem at time $t = 0.8$.

length scale are given at the inlet. The mean pressure corresponding to the isentropic outlet Mach number $M_{2i} = 1.162$ is given at the outlet. The Reynolds number related to the blade chord and outlet density and velocity is $Re = 848000$.

The piecewise linear WLSQR reconstruction has been used both the conservative variables ρ , ρu , ρw , e as well as for the turbulent quantities ρk , and $\rho \omega$. The discretisation in time was carried out by the linearized backward Euler method.

The figure 4 shows the isolines of Mach number obtained with the above mentioned method with standard weights given by eq. (10). The hybrid mesh consists of 14812 quadrilaterals inside the boundary layer and the mixing region and of 9275 triangles in the rest of the domain. It can be seen, that the WLSQR method performs very well even for this complicated mesh topology.

he

4.4 3D inviscid flow around a wing

In order to assess the performance of the WLSQR method in 3D the flow around the NACA 0012 wing has been solved. The wing is defined by two NACA 0012 profiles with chord length $c = 1$ at the root of the wing and with chord $c = 0.5$ at maximum span $z = 3$. The straight outlet edge is normal to the symmetry plane (see fig. 5 for the sketch of the wing). The flow is inviscid with angle of attack $\alpha = 0^\circ$ and inlet Mach number $M_\infty = 0.85$. The problem is considered in a rectangular domain $\Omega = [-5, 5] \times [-5, 5] \times [0, 6]$ with the inlet at the plane $x = -5$ and the outlet at $x = 5$ and with the symmetry at $z = 0$, $z = 6$, $y = \pm 5$. Since the wing is symmetric and the angle of attack is zero, the calculation has been performed only in the upper part of domain Ω with $y > 0$ and the symmetry was applied at $y = 0$ (the red domain at the fig. 5). A very simple single-block structured mesh with $100 \times 50 \times 25$ hexahedral cells created by P. Furmánek¹⁷ has been used for the calculations since it allows us to make the calculation also by other methods.

Figure 7 shows the isolines of pressure coefficient c_p obtained with:

- The one-dimensional MUSCL reconstruction with minmod limiter, where

$$u_{i+1/2,j,k}^L = u_{i,j,k} + \frac{1}{2} \text{minmod}(\Delta_{i-1/2,j,k} u, \Delta_{i+1/2,j,k} u), \quad (18)$$

$$u_{i+1/2,j,k}^R = u_{i+1,j,k} - \frac{1}{2} \text{minmod}(\Delta_{i+1/2,j,k} u, \Delta_{i+3/2,j,k} u), \quad (19)$$

where $\Delta_{i+1/2,j,k} u = u_{i+1,j,k} - u_{i,j,k}$, $u_{i+1/2,j,k}^{L/R}$ are the interpolated values of the solution at the left and right hand side of the face $i + 1/2, j, k$ and $\text{minmod}(a, b) = \text{sign}(a) \max(0, \min(|a|, \text{sign}(a)b))$.

- The one-dimensional WLSQR reconstruction, where

$$u_{i+1/2,j,k}^L = u_{i,j,k} + \frac{1}{2} \sigma_{i,j,k} \quad (20)$$

$$u_{i+1/2,j,k}^R = u_{i+1,j,k} - \frac{1}{2} \sigma_{i+1,j,k}, \quad (21)$$

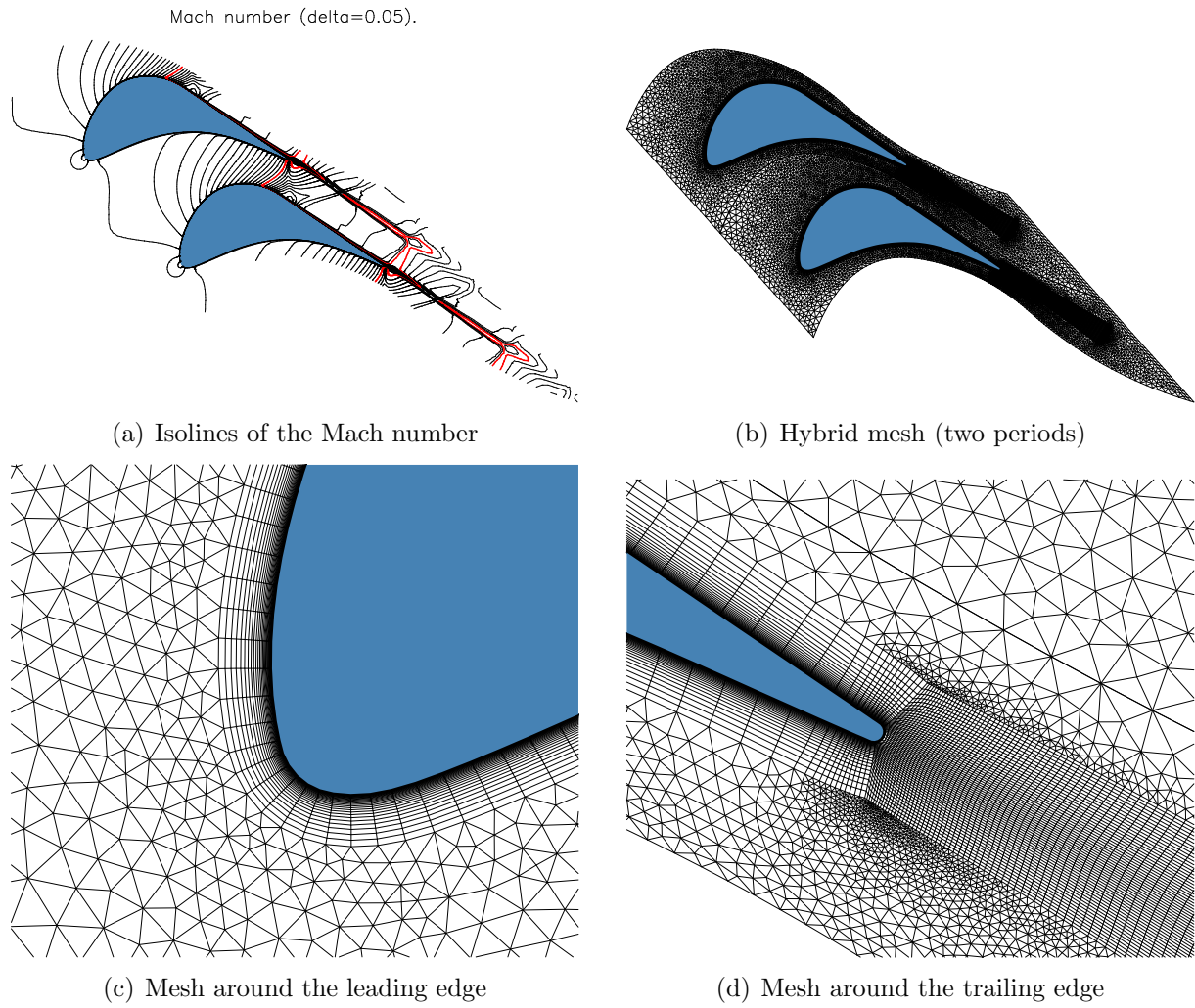


Figure 4: Hybrid mesh and isolines of Mach number in the 2D turbine cascade of Škoda Plzeň, $M_{2i} = 1.162$, $Re = 848000$.

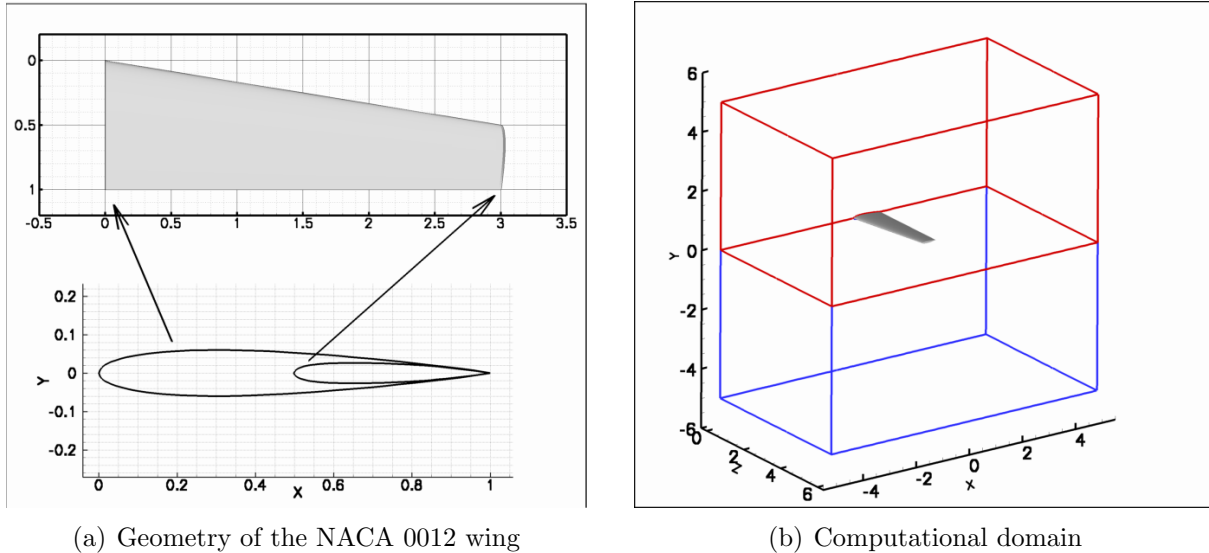


Figure 5: Geometry of the 3D NACA 0012 wing and the computational domain.

Figure 6: Isolines of the pressure coefficient c_p obtained with 3D WLSQR method.

where $\sigma_{i,j,k} = (w_{i+1/2,j,k}^2 \Delta_{i+1/2,j,k} u + w_{i-1/2,j,k}^2 \Delta_{i-1/2,j,k} u) / (w_{i+1/2,j,k}^2 + w_{i-1/2,j,k}^2)$, and $w_{i+1/2,j,k} = 1 / [(\Delta_{i+1/2,j,k} u)^4 + 1]$.

- The multidimensional WLSQR reconstruction described in this article.

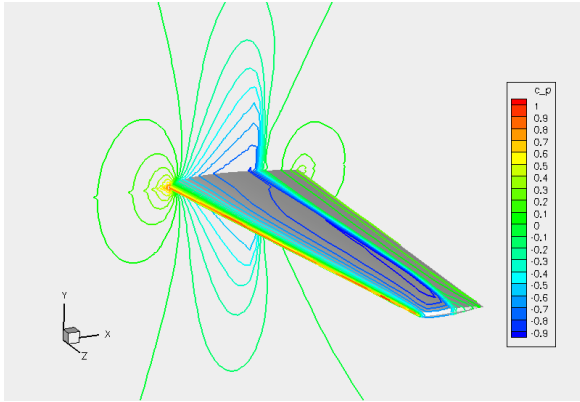
The discretization in time was achieved by the backward Euler method with factorized linearization.

One can see that there is very small difference between those methods in the distribution of c_p . Figure 7 documents small overshoot at the shock wave generated by the WLSQR method, however, the overshoot is small and the method seems to be stable. On the other hand, the 3D WLSQR method outperforms both MUSCL and 1D WLSQR in the convergence to steady state (see fig. 7). The steady residual is evaluated here as the L^2 norm of the time derivative of density.

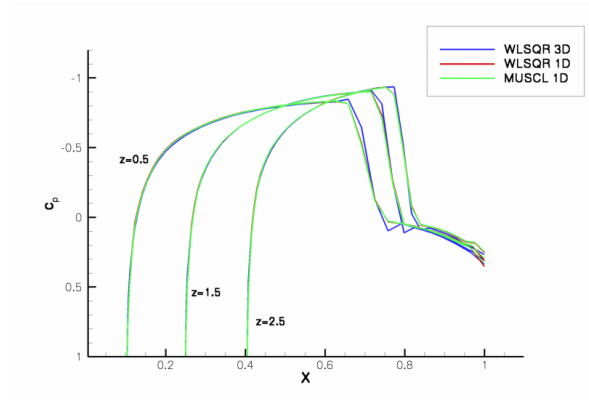
5 CONCLUSION

This article documents several properties of the WLSQR method. First of all, the method is simply extensible even for piecewise parabolical reconstructions with unstructured meshes (see the 2D GAMM channel example). Moreover, the method can be used for the solution of industrial problems such as turbulent flows with shock waves in complex geometry. Some preliminary results for 3D flows has been also presented.

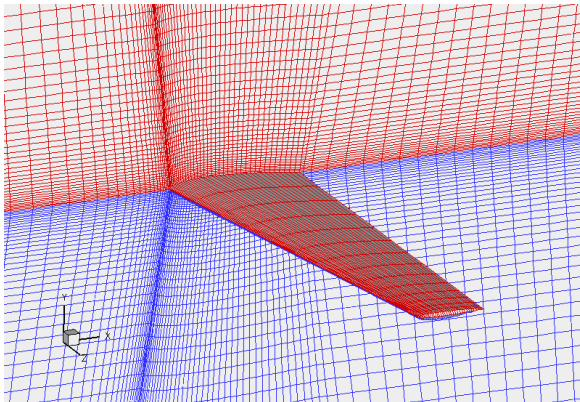
On the other hand, the choice of the weights is not universal for all types of flow problems. For example, in order to be able to solve complicated 2D Riemann problem, it



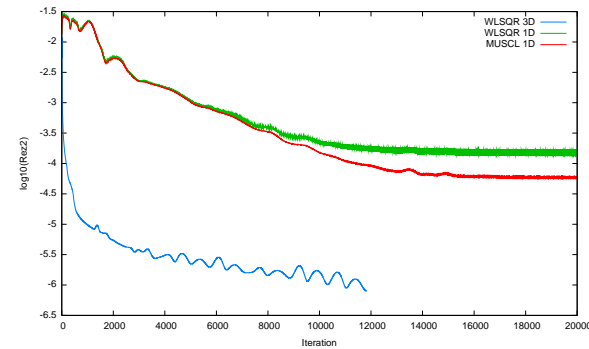
(a) Pressure coefficient obtained with WLSQR.



(b) Distribution of c_p for $z = 0.5, 1.5,$ and 2.5 for three different interpolations.



(c) 3D mesh around the wing.



(d) Convergence history.

Figure 7: The pressure coefficient c_p obtained with the 3D WLSQR method, the comparison of distribution of c_p at three cuts $z = 0.5, z = 1.5,$ and $z = 2.5$ for three different interpolation techniques, mesh around the wing and the convergence history for time derivative of the density.

was necessary to change a bit the definition of the weights. Nevertheless, the weights were chosen using the same principles as for the original weights.

Acknowledgments Partial support of the project No. 201/05/0005 of the Grant Agency of the Czech Republic, Research Plan MSM No. 6840770010 is acknowledged.

References

- [1] M. Feistauer, J. Felcman, and I. Straškraba. *Mathematical and Computational Methods for Compressible Flow*. Numerical Mathematics and Scientific Computation. Oxford University Press (2003). ISBN 0-19-850588-4.
- [2] A. Harten, B. Enquist, S. Osher, and S. Chakravarthy. Uniformly high order essentially non-oscillatory schemes iii. *Journal of Computational Physics*, 71, 231–303 (1987).
- [3] G.-S. Jiang and C.-W. Shu. Efficient implementation of weighted ENO schemes. *Journal of Computational Physics*, 126, 202–228 (1996).
- [4] A. Harten and S. R. Chakravarthy. Multi-dimensional ENO schemes for general geometries. Technical Report 91-76, ICASE (1991).
- [5] O. Friedrich. Weighted essentially non-oscillatory schemes for the interpolation of mean values on unstructured grids. *Journal of Computational Physics*, 144(1), 194–212 (1998).
- [6] J. Fůrst and K. Kozel. Numerical solution of transonic flows through 2D and 3D turbine cascades. *Computing and Visualization in Science*, 4(3), 183–189 (2002).
- [7] J. Fůrst and K. Kozel. Second and third order weighted ENO scheme on unstructured meshes. In F. Benkhaldoun and R. Vilsmeier, editors, *Finite Volumes for Complex Applications. Problems and Perspectives*. Hermes (2002).
- [8] J. Fůrst. A finite volume scheme with weighted least square reconstruction. In S. R. F. Benkhaldoun, D. Ouazar, editor, *Finite Volumes for Complex Applications IV*, pages 345–354. Hermes Science (2005). ISBN 1-905209-48-7.
- [9] J. Fůrst. A weighted least square scheme for compressible flows (2005). Submitted to "Flow, Turbulence and Combustion".
- [10] S. Osher and S. Chakravarthy. Upwind schemes and boundary conditions with applications to Euler equations in general geometries. *J. Comp. Phys.*, (50), 447–481 (1983).

- [11] K. H. Kim, C. Kim, and O.-H. Rho. Methods for the accurate computations of hypersonic flows i. AUSMPW+ scheme. *Journal of Computational Physics*, (174), 38–80 (2001).
- [12] J. Fürst. *Numerical modeling of the transonic flows using TVD and ENO schemes*. Ph.D. thesis, ČVUT v Praze and l’Université de la Méditerranée, Marseille (2001).
- [13] J. Fürst. Numerical solution of inviscid and viscous flows using modern schemes and quadrilateral or triangular mesh. In M. Beneš, editor, *Proceedings of the Czech-Japanese Seminar in Applied Mathematics*. Czech Technical University in Prague (2004).
- [14] A. Kurganov and E. Tadmor. Solution of two-dimensional Riemann problems without riemann solvers. *Numerical Methods for Partial Differential Equations*, (18), 548–608 (2002).
- [15] J. Dobeš and H. Deconinck. Second order blended multidimensional residual distribution scheme for steady and unsteady computations. *Journal of Computational and Applied Mathematics (JCAM)* (2005). Submitted.
- [16] J. C. Kok. Resolving the dependence on free stream values for the k-omega turbulence model. Technical Report NLR-TP-99295, NLR (1999).
- [17] P. Furmánek, J. Fürst, K. Kozel, and P. Mastný. Numerical solution of transonic flow over an airfoil. In K. K. J. Příhoda, editor, *Kolokvium "Dynamika Tekutin 2005"*, pages 41–44. IT CAS CZ (2005). ISBN 80-85918-94-3.